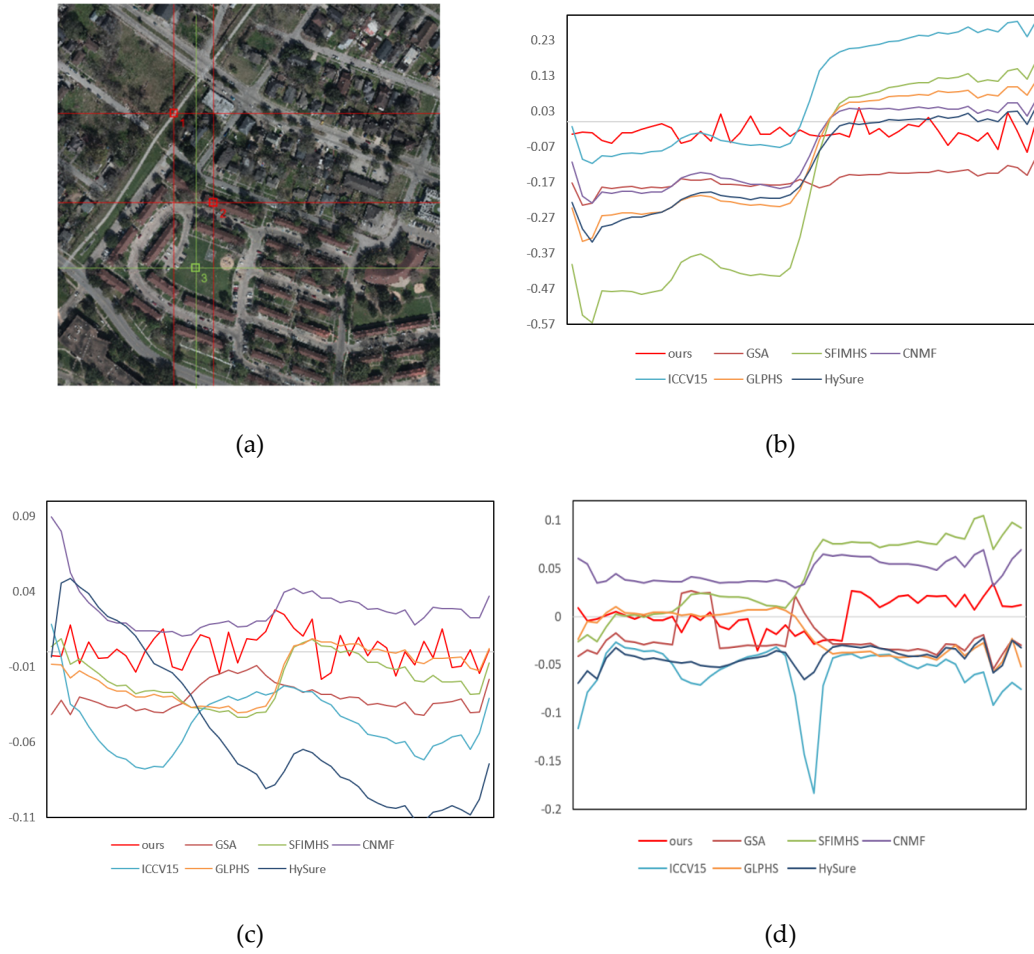


# Supplementary Materials: Hyperspectral and Multispectral Image Fusion by deep neural network in a self-supervised manner

Jianhao Gao , Jie Li and Menghui Jiang

## 1. Spectral Difference Curve of Different Ground Objects

We select three pixels from different ground objects, which are respectively roads, buildings and grassland, and display their spectral difference curves in Figure 1. The spectral difference curve is the difference curve between curves of the selected pixel and corresponding ground truth pixel. We can observe from Figure 1 that the spectral difference curves of our results are closest to 0, indicating that our results have most accurate spectral information.

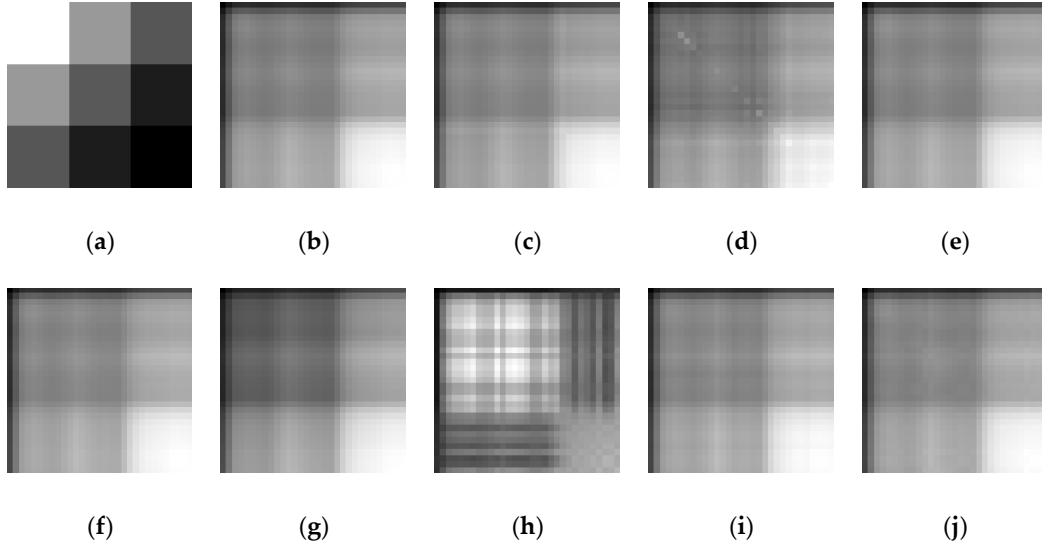


**Figure S1.** Curve of spectral difference between selected pixels and ground truth (a) locations of three selected pixels; (b) Spectral difference curve of Pixel 1 (Road); (c) Spectral difference curve of Pixel 2 (Building); (d) Spectral difference curve of Pixel 3 (grass).

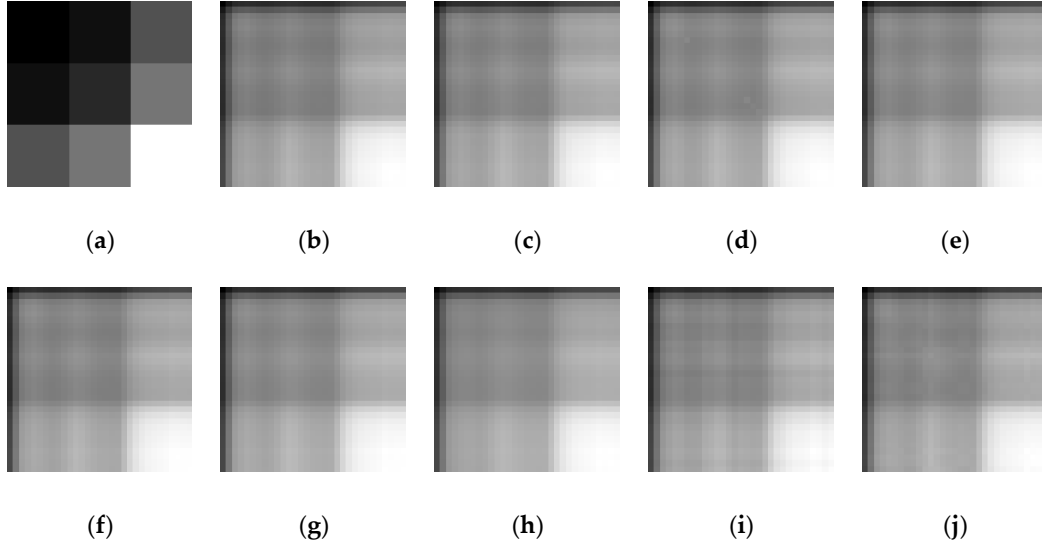
## 2. Visualization of Covariance Matrix

We visualize the covariance matrix of HR MSI, LR HSI, ground truth and results of all methods in Figure 2-6. All methods perform well in experiments with simulated HR

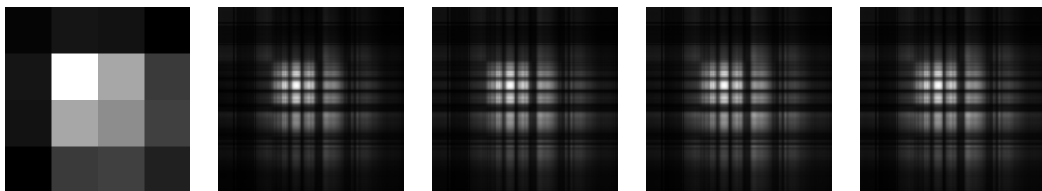
MSI. However, when it comes to experiments with real HR MSI, results of our method have the closest covariance matrix to that of ground truth.

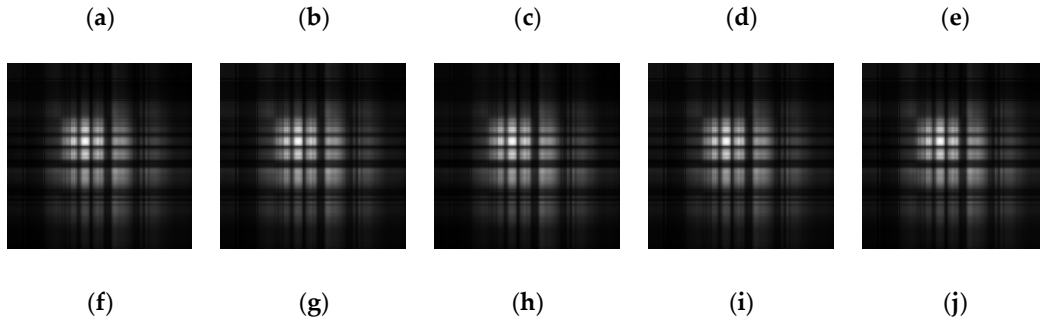


**Figure S2.** co-variance matrix of CAVE dataset experiment with real HR MSI. (a) HR MSI; (b) LR HSI; (c) GSA; (d) SFIMHS; (e) GLPHS; (f) CNMF; (g) ICCV15; (h) HySure; (i) ours; (j)HR HSI;.

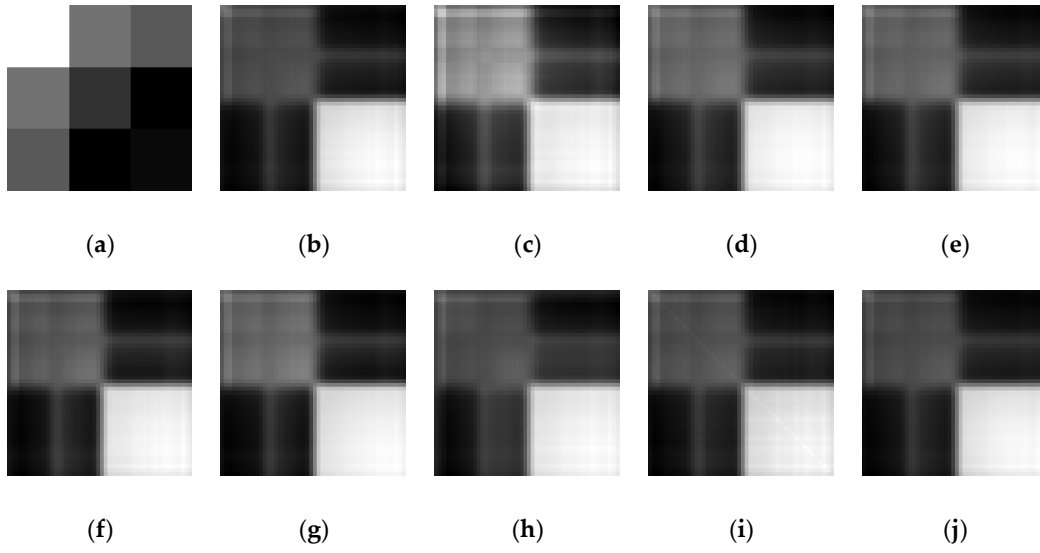


**Figure S3.** co-variance matrix of CAVE dataset experiment with simulated HR MSI. (a) HR MSI; (b) LR HSI; (c) GSA; (d) SFIMHS; (e) GLPHS; (f) CNMF; (g) ICCV15; (h) HySure; (i) ours; (j)HR HSI;.

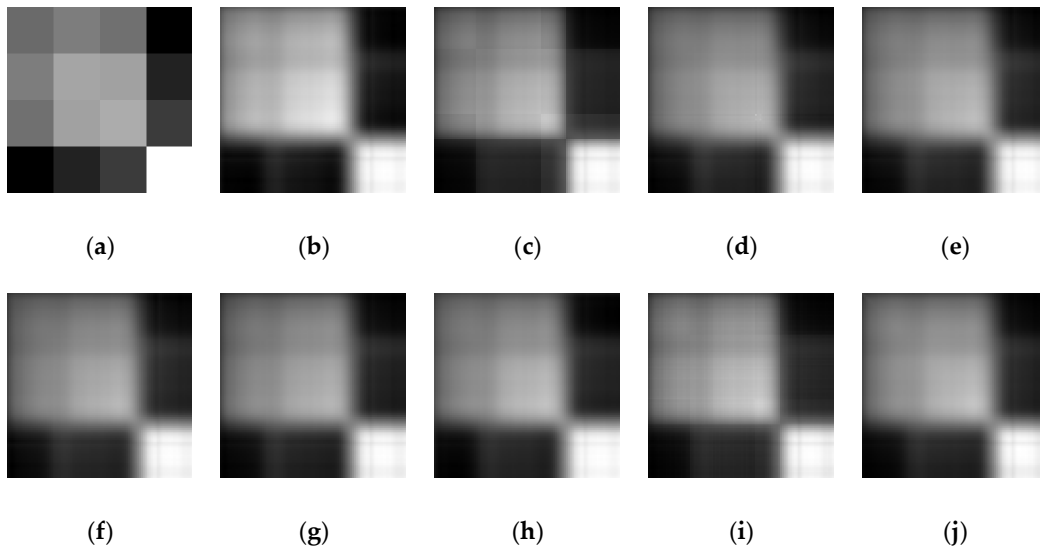




**Figure S4.** co-variance matrix of Washington DC dataset experiment with simulated HR MSI. (a) HR MSI; (b) LR HSI; (c) GSA; (d) SFIMHS; (e) GLPHS; (f) CNMF; (g) ICCV15; (h) HySure; (i) ours; (j)HR HSI;.



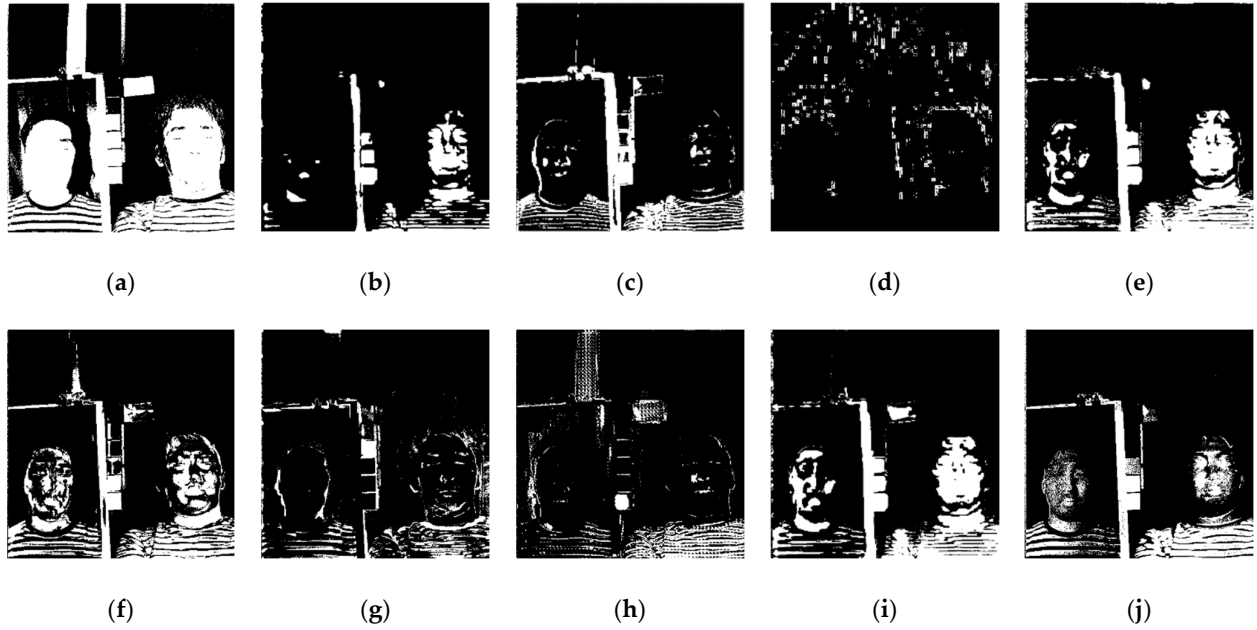
**Figure S5.** co-variance matrix of Houston 2018 dataset experiment with real HR MSI. (a) HR MSI; (b) LR HSI; (c) GSA; (d) SFIMHS; (e) GLPHS; (f) CNMF; (g) ICCV15; (h) HySure; (i) ours; (j)HR HSI;.



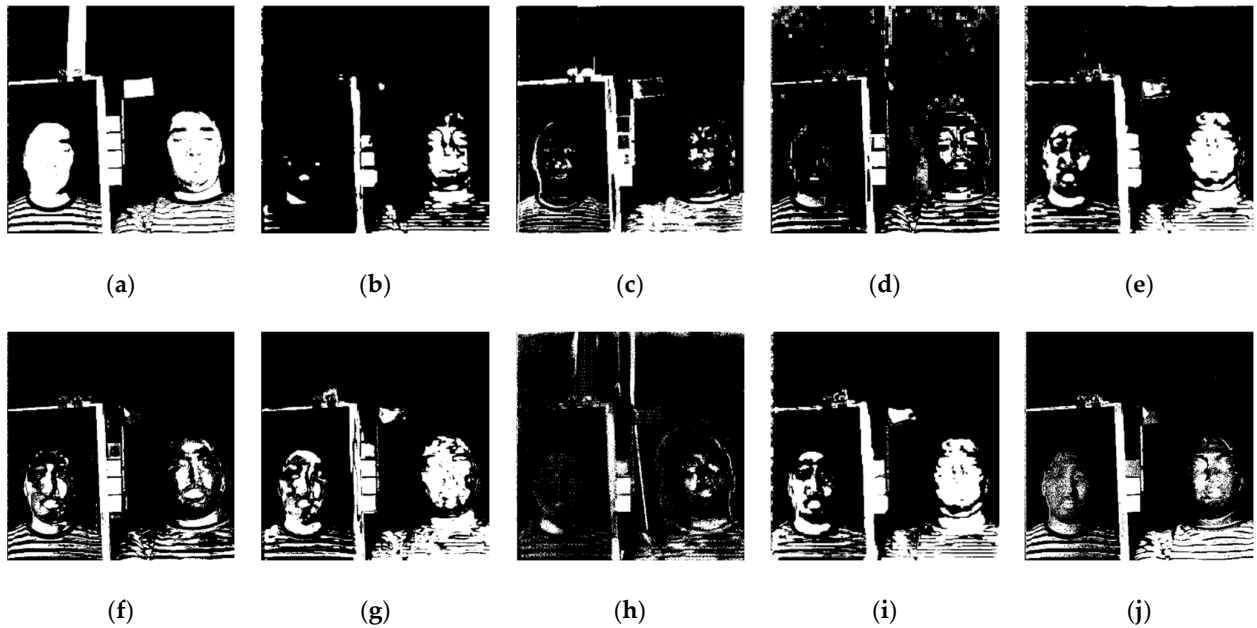
**Figure S6.** co-variance matrix of Pavia dataset experiment with simulation HR MSI. (a) HR MSI; (b) LR HSI; (c) GSA; (d) SFIMHS; (e) GLPHS; (f) CNMF; (g) ICCV15; (h) HySure; (i) ours; (j)HR HSI;.

### 3. RX Detection Maps of Results

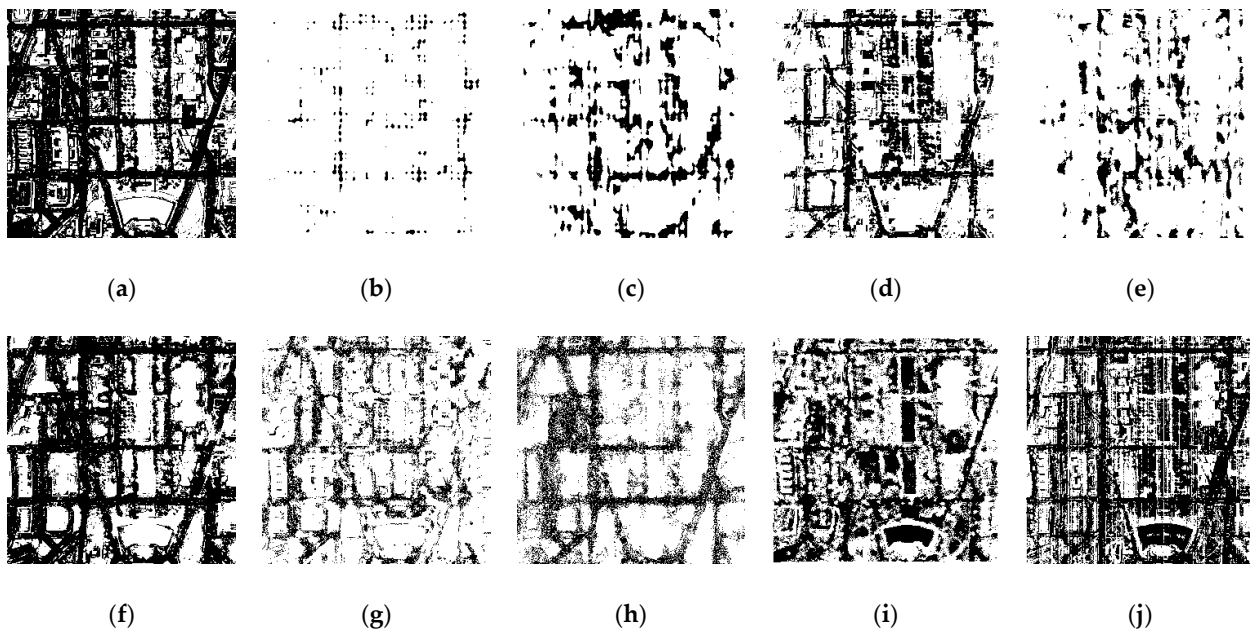
We supplement the RX detection maps of all methods in Figure 7-11. We can observe that results of the proposed method can obtain more accurate detection results compared with other methods (see Figure 7-10) and resist the disturbance of noise compared with HR HSI (see Figure 11)



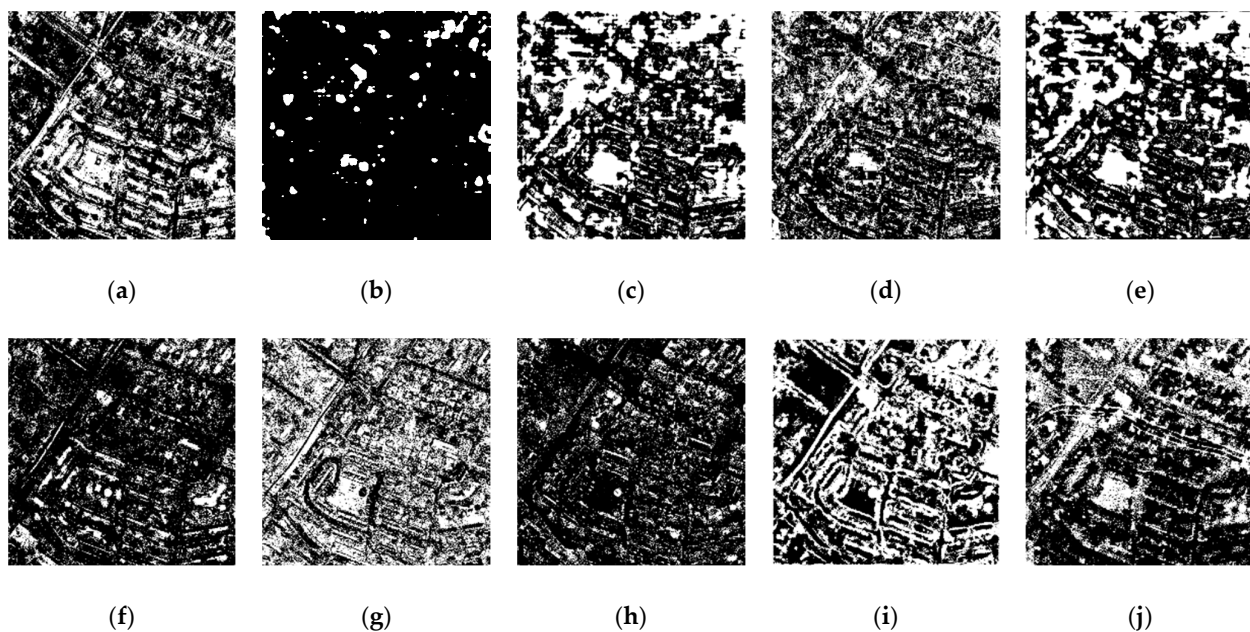
**Figure S7.** RX map of CAVE dataset experiment with real HR MSI. (a) HR MSI; (b) LR HSI; (c) GSA; (d) SFIMHS; (e) GLPHS; (f) CNMF; (g) ICCV15; (h) HySure; (i) ours; (j)HR HSI;



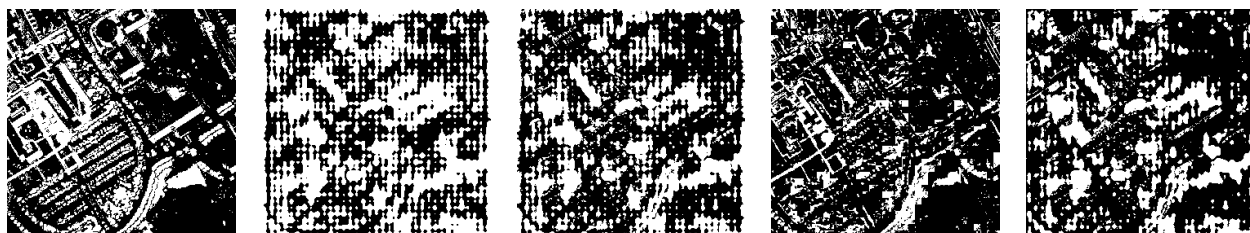
**Figure S8.** RX map of CAVE dataset experiment with simulated HR MSI. (a) HR MSI; (b) LR HSI; (c) GSA; (d) SFIMHS; (e) GLPHS; (f) CNMF; (g) ICCV15; (h) HySure; (i) ours; (j)HR HSI;.



**Figure S9.** RX map of WashingtonDC dataset experiment with real HR MSI. (a) HR MSI; (b) LR HSI; (c) GSA; (d) SFIMHS; (e) GLPHS; (f) CNMF; (g) ICCV15; (h) HySure; (i) ours; (j)HR HSI;.



**Figure S10.** RX map of Houston 2018 dataset experiment with simulated HR MSI. (a) HR MSI; (b) LR HSI; (c) GSA; (d) SFIMHS; (e) GLPHS; (f) CNMF; (g) ICCV15; (h) HySure; (i) ours; (j)HR HSI;.



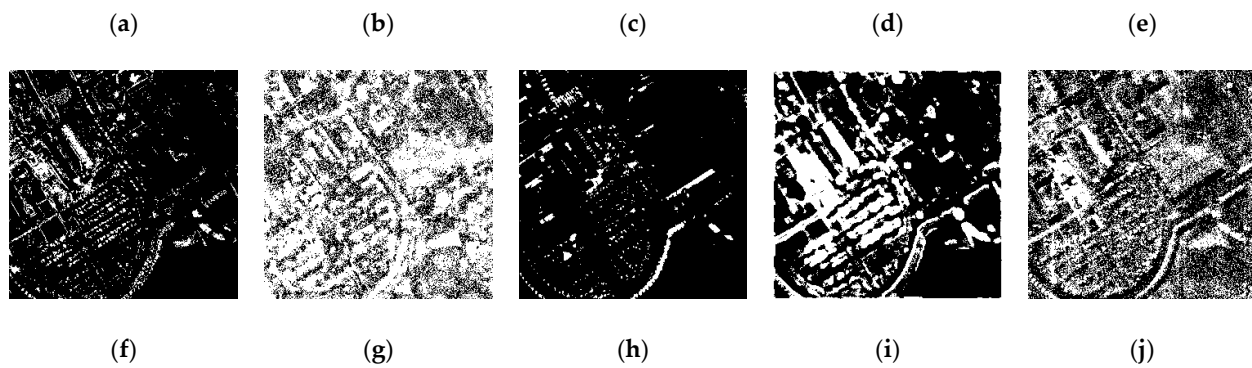


**Figure S11.** RX map of Pavia dataset experiment with simulated HR MSI. (a) HR MSI; (b) LR HSI; (c) GSA; (d) SFIMHS; (e) GLPHS; (f) CNMF; (g) ICCV15; (h) HySure; (i) ours; (j)HR HSI;